Impact of past climate warming on genomic diversity and demographic history of collared lemmings across the Eurasian Arctic

Vadim B. Fedorov[a,1], Emiliano Trucchi[b,c], Anna V. Goropashnaya[a], Eric Waltari[d,2], Susan Erin Whidden[a,3], and Nils Chr. Stenseth[b,1]

[a]Institute of Arctic Biology, University of Alaska Fairbanks, Fairbanks, AK 99775-7000; [b]Centre for Ecological and Evolutionary Synthesis, Department of Biosciences, University of Oslo, Blindern, 0316 Oslo, Norway; [c]Department of Life and Environmental Sciences, Marche Polytechnic University, 60131 Ancona, Italy; and [d]Department of Biology, City College of New York, New York, NY 10031

Contributed by Nils Chr. Stenseth, December 18, 2019 (sent for review August 7, 2019; reviewed by Heikki Henttonen and Jeremy B. Searle)

The Arctic climate was warmer than today at the last interglacial and the Holocene thermal optimum. To reveal the impact of past climate-warming events on the demographic history of an Arctic specialist, we examined both mitochondrial and nuclear genomic variation in the collared lemming (*Dicrostonyx torquatus*, Pallas), a keystone species in tundra communities, across its entire distribution in northern Eurasia. The ancestral phylogenetic position of the West Beringian group and divergence time estimates support the hypothesis of continental range contraction to a single refugial area located in West Beringia during high-magnitude warming of the last interglacial, followed by westward recolonization of northern Eurasia in the last glacial period. The West Beringian group harbors the highest mitogenome diversity and its inferred demography indicates a constantly large effective population size over the Late Pleistocene to Holocene. This suggests that northward forest expansion during recent warming of the Holocene thermal optimum did not affect the gene pool of the collared lemming in West Beringia but reduced genomic diversity and effective population size in all other regions of the Eurasian Arctic. Demographic inference from genomic diversity was corroborated by species distribution modeling showing reduction in species distribution during past climate warming. These conclusions are supported by recent paleoecological evidence suggesting smaller temperature increases and moderate northward forest advances in the extreme northeast of Eurasia during the Late Pleistocene-to-Holocene warming events. This study emphasizes the importance of West Beringia as a potential refugium for cold-adapted Arctic species under ongoing climate warming.

Beringia | climate warning | interglacial | Holocene optimum | mitogenome

In polar regions, the magnitude of recent climate warming is larger than in other parts of the Earth (1) and this amplified warming significantly impacts cold-adapted Arctic and Antarctic biotas (2–4). An informative approach to predict the biological consequences of ongoing Arctic warming in the near future is to assess past biotic responses to the Late Quaternary warming events. In the recent past, Arctic climate was warmer than today at both the last interglacial (the Eemian, 130 to 110 thousand years ago; kyr) and the Holocene thermal maximum between 10 and 3 kyr (1, 5). Species distribution shifts, often associated with local extinction, were the most common response to the Late Quaternary environmental change (6). During warming events, Arctic tundra was reduced as boreal forest communities advanced to the north and was simultaneously restricted from northward retreat by the seacoast (1, 5). Contraction of distribution ranges is expected to reduce effective population size and genetic diversity, making Arctic terrestrial species vulnerable to climate warming. However, demographic and genetic effects of past warming events on a continental scale across the Eurasian Arctic remain largely unknown.

Collared lemmings (*Dicrostonyx*), the northernmost rodents and keystone species in the Arctic tundra communities, evolved and have long been associated with cold and dry treeless tundra landscapes (7–10). The fossil record shows that during glacial periods, collared lemmings expanded their distribution thousands of kilometers to the south and west while in warm periods of the past and present interglacials their range was restricted to the Arctic (11). Previous studies have revealed the low mitochondrial (mt)DNA diversity in the Eurasian collared lemmings, suggesting reductions in long-term effective population size which most likely resulted from range contractions during the Late Quaternary warming events (12, 13). However, this explanation remains ambiguous due to the obscure position of the root in phylogeny, uncertain calibration of the molecular clock, and limited sampling in the extreme northeast of the Eurasian Arctic. Nevertheless, recent paleogenetic studies (14, 15) support the significant impact of environmental change in the Late Quaternary on the genetic diversity and demographic history of the collared

Significance

Ongoing climate warming significantly impacts cold-adapted Arctic biota. One way to predict the biological consequences of Arctic warming in the future is to investigate biotic responses to past warming events. We use variation in mitochondrial and nuclear genomes in the collared lemming, a keystone species of the food web in tundra, to reconstruct demographic changes as a response to warming of the last interglacial and Holocene thermal optimum. We show that environmental change during Late Quaternary climate warming contracted distribution range, reduced effective population size, and decreased genetic diversity across the Eurasian Arctic except for West Beringia, a region in the extreme northeast of Eurasia. Thus, West Beringia represents a potential refugium for terrestrial Arctic species under ongoing climate warming.

Author contributions: V.B.F., E.W., and N.C.S. designed research; V.B.F., E.T., A.V.G., and S.E.W. performed research; V.B.F., E.T., A.V.G., and E.W. analyzed data; and V.B.F., E.T., A.V.G., E.W., and N.C.S. wrote the paper.

Reviewers: H.H., Natural Resources Institute Finland; and J.B.S., Cornell University.

The authors declare no competing interest.

Data deposition: The DNA sequences reported in this paper have been deposited in the GenBank database under BioProject ID PRJNA599530.

[1]To whom correspondence may be addressed. Email: vfedorov@alaska.edu or n.c.stenseth@mn.uio.no.

[2]Present address: Chan Zuckerberg Biohub, San Francisco, CA 94158.

[3]Present address: Faculty of Forestry and Environmental Management, University of New Brunswick, Fredericton, NB E3B 5A3, Canada.

This article contains supporting information online at https://www.pnas.org/lookup/suppl/doi:10.1073/pnas.1913596117/-/DCSupplemental.

First published January 27, 2020.

lemming. Synchronous genetic replacements in populations of the collared lemming implied repeated extinctions and recolonizations associated with environmental fluctuations over the last 50 kyr in western Eurasia (15). On a local scale, an ancient DNA study in a single population of the collared lemming from western Eurasia detected a drastic decrease in genetic diversity after the last glacial maximum (22 kyr) and over the Holocene, suggesting a pronounced demographic reduction during warming events (14).

To reveal the impact of past climate-warming events on the demographic history of Arctic species, we examined both mitochondrial and nuclear genomic diversity in collared lemming populations from across its entire modern distribution (Fig. 1). We put special emphasis on sampling across the Chukotka Peninsula in the eastern part of the species distribution to include West Beringia, a geographic region with distinct environmental history (16) that has been proposed as a possible location of warm interglacial refugium (17). On a continental scale, we reconstructed a calibrated phylogeny and estimated divergence times to assess possible range contraction to a single refugium as a species-wide response to large-magnitude climate warming during the last interglacial. On a regional scale, we estimated genomic diversity, reconstructed demographic history, and compared estimates across geographic regions with different environmental histories to reveal the impact of the Holocene climate warming. To validate demographic events reflected in current genomic variation, we used independent evidence from species distribution modeling to infer changes in species range during past warming events.

Results and Discussion

Phylogeographic Structure across the Eurasian Arctic. The maximum-credibility tree based on mitogenome sequences (Fig. 2) shows the main phylogenetic division across the Bering Strait separating the Eurasian and North American lemmings. In Eurasia, there are 5 major monophyletic groups of haplotypes corresponding to different geographic regions. This indicates a clear association between phylogenetic relationships and the geographic origin of the haplotypes. The most ancient phylogenetic division separating the West Beringian group and all other Eurasian phylogroups (Pechora, P; Yamal, Y; Taymyr, T; Yana-Kolyma, YK) is across the Kolyma River (Figs. 1 and 2). The discrete phylogeography analysis suggested West Beringia (WB) as the most likely (Bayes factor 2.8 to 4.4) location of the ancestor of all lineages in Eurasia.

The nuclear genome phylogenies are congruent with the phylogeographic structure based on variation in mitogenome sequences. The Neighbor-Net (Fig. 3) based on the number of nucleotide differences (p distances) across concatenated restriction site-associated DNA (RAD) loci shows 4 groups with allopatric distribution in the Eurasian Arctic regions and the most divergent outgroup clustering all individuals of the North American lemmings *Dicrostonyx groenlandicus*. Similar to the mitogenome phylogeny, the West Beringian cluster is the closest to the outgroup among the Eurasian lineages in a TreeMix based on allele frequencies (Fig. 4*A*). The TreeMix analysis also suggested a maximum of 2 events of secondary contact and admixture between divergent groups (Fig. 4*A*). A fineRADstructure analysis (Fig. 4*B*) provides further support for the phylogeographic structure revealed by the Neighbor-Net and TreeMix reconstructions. The coancestry matrix summarizing the nucleotide differences among individuals across all RAD loci (Fig. 4*B*) shows more common ancestry among alleles within a geographic region (Y, T, YK, WB) as compared with individuals from different regions. However, consistent with the migration event detected by TreeMix, there is indication of admixture in the population from Taymyr, where individuals show high coancestry with each other but also with lemmings from other regions.

Our study shows a clear phylogeographic structure associated with significant reciprocal monophyly in the Eurasian collared lemmings. Notably, our present results demonstrate congruence between geographic patterns of mitochondrial and nuclear genomic variation and provide statistical support for the West Beringian location of the ancestor of all Eurasian lineages. It was previously proposed on the basis of limited mtDNA nucleotide divergence that the distribution of the collared lemming in Eurasia was contracted to a single refugium, possibly located in West Beringia, during climate-warming events in one of the interglacials (17). However, this hypothesis has been complicated by the lack of statistical support for the tree topology and imprecise estimates of divergence time. Our mitogenome molecular clock, calibrated by the first occurrence of fossil records in North America, dates the most ancient phylogenetic division separating the basal West Beringian group from other Eurasian lineages (104 kyr; 95% highest posterior density [HPD] 74 to 142 kyr) to the beginning of the last glacial period (110 to 10 kyr) and after the last interglacial (130 to 110 kyr). The time points for our calibration are based on the first occurrence of *Dicrostonyx*

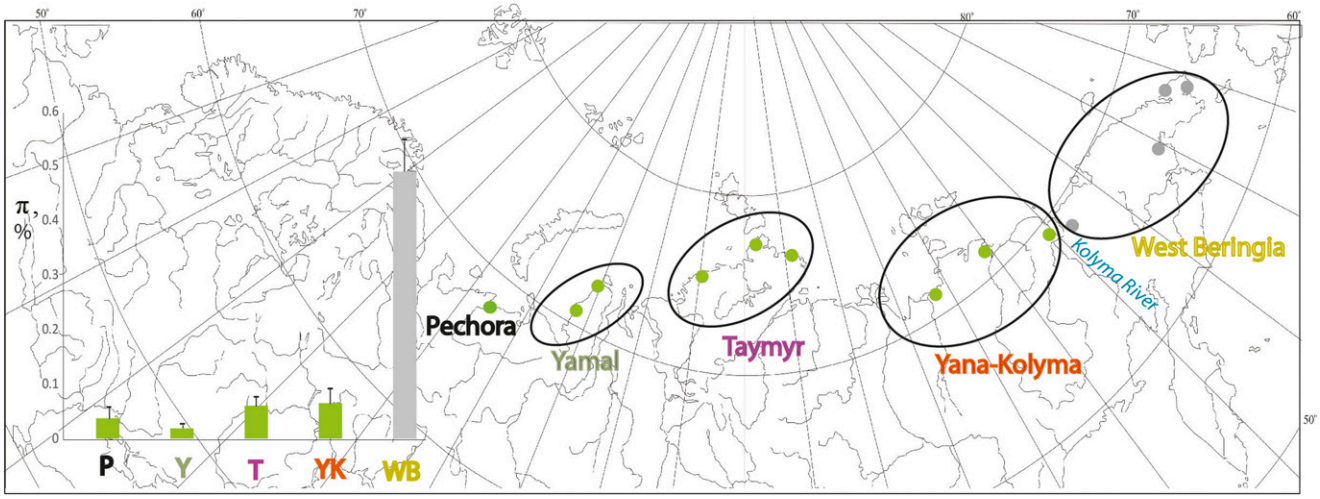

Fig. 1. Sampling locations and geographic ranges of the phylogeographic groups (Figs. 2 and 3) of Eurasian collared lemmings. Bars show mitogenome nucleotide diversity and its SD estimates in regions (green) affected by northward forest expansion during the Holocene thermal maximum compared with West Beringia (gray) with limited forest advances.

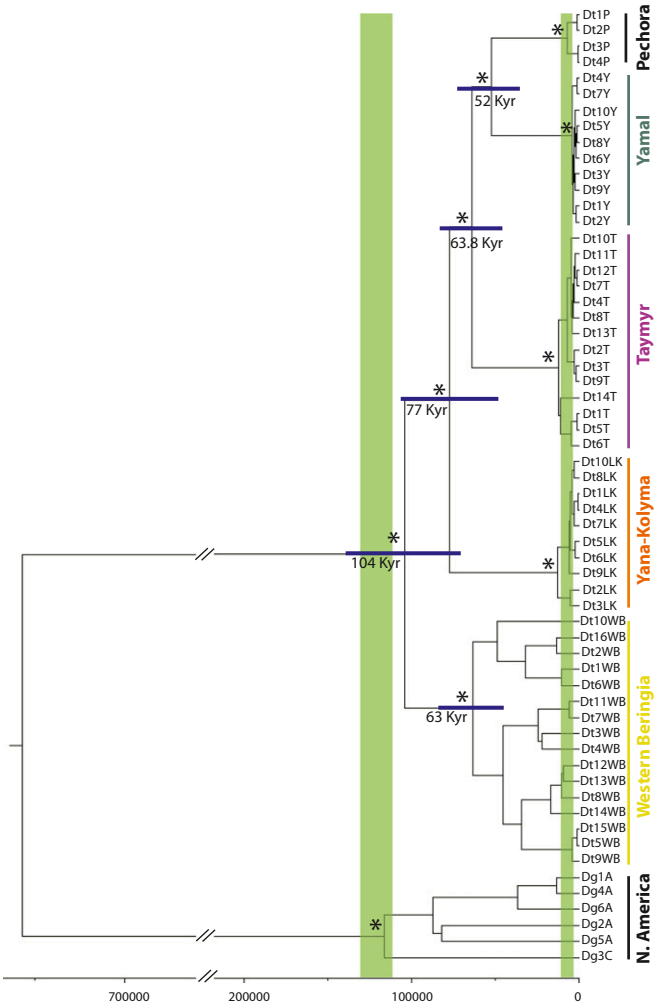

Fig. 2. Maximum-credibility tree based on mitogenome sequences of collared lemmings. Horizontal bars represent the 95% CI for node divergence time shown by the numbers; asterisks indicate major nodes supported with posterior probability 1. Information about the sequences is provided in *SI Appendix*, Table S1. Green bars show warming periods of the last interglacial (130 to 110 kyr) and Holocene thermal maximum (10 to 3 kyr).

fossils in North America at 700 to 740 kyr (18, 19) and the latest North American record of its ancestor, *Predicrostonyx* (20), dated to 1.5 to 1.7 My (21). It was suggested that a short-term mtDNA substitution rate estimated over time of less than 1 to 2 My is considerably higher than the rate inferred from species phylogeny (22). Although a very high short-term substitution rate was previously reported for 2 species of arvicoline rodents (23, 24), our phylogenetic rate estimate of 5.6E-8 substitutions per site per y (95% HPD 4.0E-8 to 7.3E-8), calibrated using the fossil-based time points, is similar to the tip rate of 6.0E-8 obtained from ancient mtDNA over just 22 kyr under the "open population with bottleneck" model for collared lemmings from Pechora (14), suggesting a minor bias in our substitution rate estimate due to time dependency. Taken together, the tree topologies and divergence time estimates support the hypothesis of range contraction to West Beringia in the last interglacial, followed by recolonization of northern Eurasia during the last glacial period. Even considering a mitochondrial substitution rate 4 times higher than we estimated in the collared lemming [as in the case of *Microtus* (23, 24)], the divergence between the West Beringian and other Eurasian mitogenomes is consistent with the recolonization from West Beringia in the last glacial period (110 to 10 kyr). Consistently, species distribution models predict about 50% habitat loss during the warming of the last interglacial relative to the present collared lemming distribution in Eurasia and 80% relative to the last glacial maximum, with suitable habitats persisting in West Beringia (*SI Appendix*, Fig. S2). Actual habitat loss likely exceeded this estimate due to inundation of Arctic land as a result of sea-level rise during the last interglacial warming (25).

Support for the significance of West Beringia as a warm interglacial refugium for cold-adapted species associated with a treeless environment comes from recent advances in the paleoecology of the Eurasian Arctic. Paleoclimate reconstructions show that the climatic optimum during the last interglacial was the warmest event of at least the past 250 kyr and this warmth strongly affected the Arctic biota (5). Terrestrial records suggest that the Arctic amplification produced last interglacial summer temperature anomalies 4 to 8 °C above present over the most of the Eurasian Arctic but a smaller increase of 2 to 4 °C was inferred in West Beringia (5). The last interglacial increase in summer temperature promoted the northward boreal forest expansion with tree line reaching the Arctic Ocean coastline and likely eliminating tundra from the landscape across the European (26, 27) and most of the Siberian Arctic (28, 29). Two collared lemming fossil assemblages stratigraphically separated by a fossil-wood horizon representing a pronounced warm event of the interglacial were reported in the Yana-Kolyma region (30). This finding provides direct paleontological evidence that the presence of the collared lemming was interrupted by the northward forest expansion during the warm interglacial. The climate reconstructions for West Beringia demonstrate a less pronounced increase in summer temperature than inferred for the Arctic regions to the west of the Kolyma River during the last interglacial (5, 31). Although the extent of

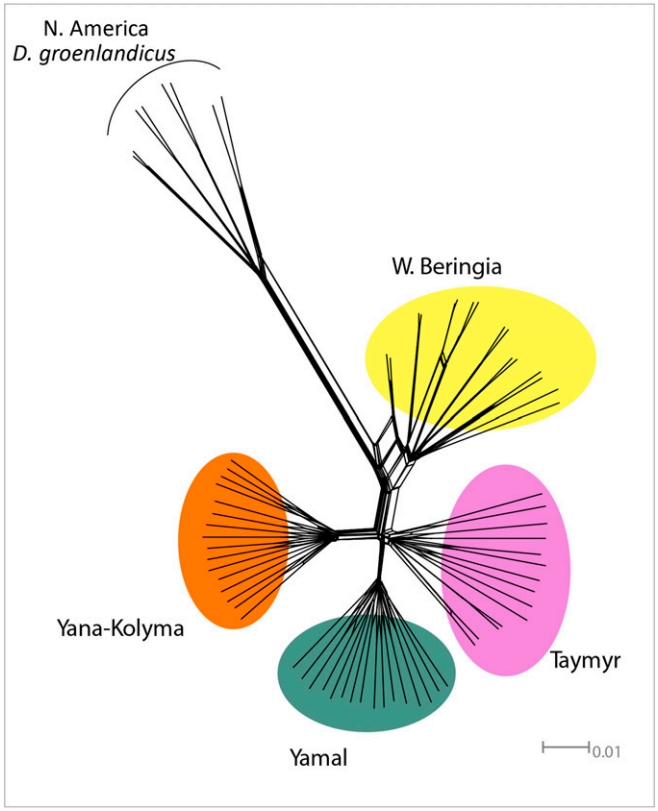

Fig. 3. Neighbor-Net tree based on nucleotide differences across concatenated RAD loci. All phylogeographic groups are supported (bootstrap > 95%).

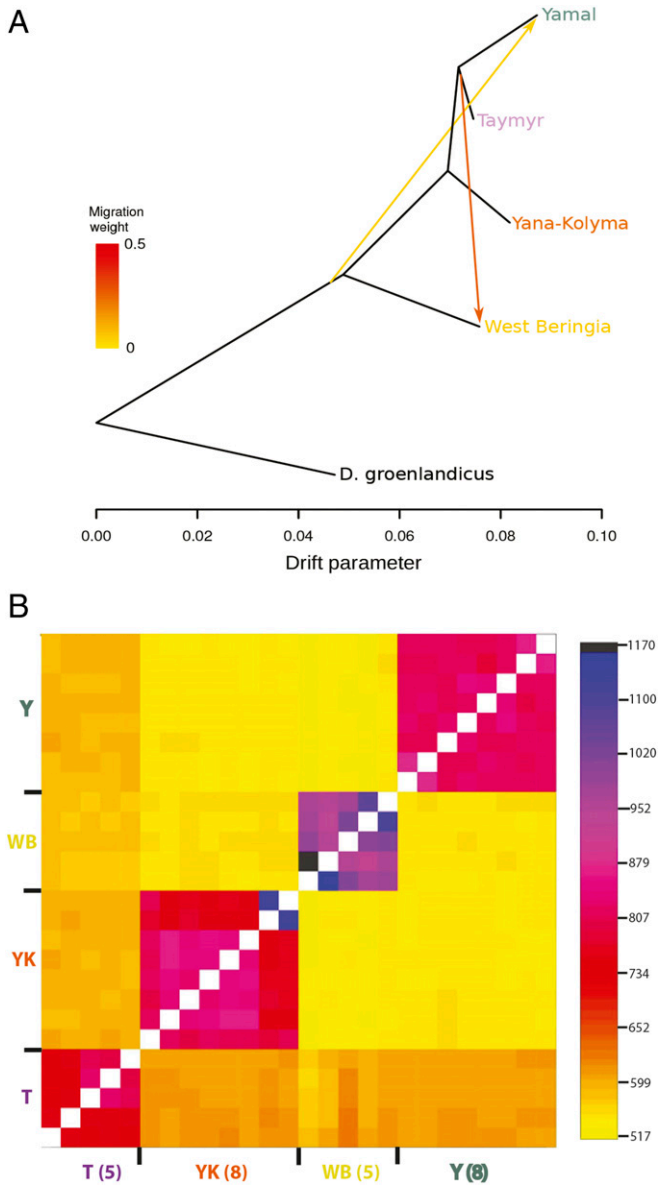

Fig. 4. Genetic differentiation across Eurasia revealed by nuclear genome variation in collared lemmings. (*A*) The TreeMix reconstruction based on allele frequencies of RAD loci. Arrows indicate 2 events of admixture. (*B*) The coancestry matrix summarizing the nucleotide differences among individuals across all RAD loci in the 4 Eurasian phylogeographic groups. The color scale indicates coancestry as the number of loci for any 2 individuals more similar to each other than to any other individual. Geographic regions are designated as in Table 1 and Fig. 1 with sampling size in parentheses.

tree line advance in West Beringia during the last interglacial optimum remains under debate (16), pollen records indicate that a tree line shifted 150 km north from its current position (16, 32) but was still located 265 km south of the Arctic coast. The biome reconstructions suggest that treeless tundra was an important landscape element in West Beringia during the last interglacial (16).

A recent paleogenetic study of the collared lemming by Palkopoulou et al. (15) identified 5 mitochondrial lineages that succeeded each other over the last 50 kyr across western Eurasia, reflecting repeated population extinction and recolonization likely due to environmental change during the Late Quaternary. An elaborate comparison of our modern mitogenome data and paleogenetic results is complicated by shorter ancient cytochrome *b* sequences (780 bp) and relatively limited sampling of the Pleistocene fossil remains from the modern distribution range of the collared lemming (15). Nevertheless, basal phylogenetic positions and higher genetic diversity of the Late Pleistocene samples from northeastern Eurasia (15) are consistent with our conclusion that the primary interglacial refugium and source of recolonizations was likely located in West Beringia. Notably, all modern cytochrome *b* sequences belong to the mtDNA lineage (EA5) that appeared in western Eurasia at 20.5 kyr (15), thus suggesting a recent origin for the phylogeographic structure revealed by our analysis of the present-day variation in nuclear and mitogenome sequences. This scenario is not excluded by mitogenome data showing considerable overlap between 95% HPD intervals for divergence time among the 5 major phylogeographic groups (Fig. 2) and the time to the most recent common ancestor (TMRCA) in the West Beringian phylogroup (Table 1). Under the assumption of similar nucleotide diversity defining the TMRCA in the ancient West Beringian population, colonization from this genetically diverse source population followed by regional bottlenecks after the last glaciation (see next section) likely accelerated formation of the monophyletic groups observed across the modern species range. Additional studies of ancient DNA sequences from West Beringia are needed to elucidate the spatial–temporal dynamic of genetic diversity reflecting demographic history of the collared lemming.

Genetic Diversity and Demography in the Arctic Regions with Different Holocene Environmental History. To infer demographic history, we analyzed genetic diversity in the 5 Eurasian phylogeographic groups defined by the maximum-credibility tree (Figs. 1 and 2). The TMRCA in the West Beringian group (Table 1) significantly exceeds the age of the TMRCAs (i.e., post glacial) in the other 4 phylogeographic groups (P, Y, T, YK). Consistent with the differences in the age of common ancestry, mitogenome nucleotide diversity estimates in the 4 phylogeographic groups (P, Y, T, YK) to the west of the Kolyma River are at least 7.5-fold lower as compared with the West Beringian group (Fig. 1 and Table 1). Notably, the West Beringian phylogroup distributed over 1,300 km of the Arctic coast harbors a similar amount of mitogenome diversity as combined gene pools of all other populations across 3,800 km of the Eurasian Arctic. To account for the effect of population structure on the high mitogenome diversity within the West Beringian group, we excluded the fraction of mitogenome variation allocated among local populations within regions by comparing intrapopulation diversity estimates in 4 West Beringian populations and 8 populations from other regions (*SI Appendix*, Fig. S1 and Table S2). Consistent with the comparison among phylogeographic groups, nucleotide diversity estimates in the West Beringian populations (range 0.208 to 0.483%) significantly exceed ($P = 0.0084$) mitogenome diversity (range 0.015 to 0.070%) in other local populations. The westernmost population (Pechora) was excluded from further demographic analysis due to small sampling size, with only 4 individuals sampled from a single locality (Table 1). To assess the significance of demographic expansion, we used Fu's F statistic and the R_2 statistic that are the most powerful tests for detecting population growth with small sampling size (33). Estimated with the mitochondrial data, negative F-statistic values were significantly different from 0 in 2 phylogeographic groups (Y, T) west of the Kolyma (Table 1), indicating an excess of low-frequency haplotypes as compared with the expected number under constant population size, which provides evidence of population expansions. This inference is supported by significantly small values of the R_2 statistic (Table 1), indicating an excess of singleton substitutions that is consistent with demographic expansions in all 3 examined phylogroups (Y, T, YK) to the west of the Kolyma. Further support for demographic expansion comes from the Bayesian skyline plot analysis showing a sudden increase in the effective population size of females at 4 to 2 kyr in the 3 phylogeographic groups (Y, T, YK) to the west of the

Table 1. Mitogenome diversity and demographic statistics for regional samples of the Eurasian collared lemming

Group	*n*	s	h	Hd	π, %	F_s	R_2	TMRCA y, (95% HPD)
Pechora	4	9	2	0.67	0.037 ± 0.011	—	—	6,430 (2,650 to 10,700)
Yamal	10	13	9	0.98	0.019 ± 0.003	−5.170***	0.072***	4,000 (1,900 to 6,440)
Taymyr	14	43	14	1.00	0.062 ± 0.009	−6.497**	0.095*	11,720 (6,950 to 17,300)
Yana-Kolyma	10	39	9	0.98	0.065 ± 0.015	−1.501	0.095**	12,620 (7,440 to 19,100)
Pooled P, Y, T, YK	38	291	34	0.99	0.530 ± 0.021	—	—	77,091 (54,225 to 107,101)
West Beringia	16	314	15	0.99	0.491 ± 0.029	0.449	0.102	63,150 (44,900 to 87,700)

The table shows sampling size (*n*), number of segregating sites (s), number of different haplotypes (h), haplotype (Hd) and nucleotide (π, %) diversities, demographic expansion statistics (F_s and R_2), and time of the most recent common ancestor in phylogeographic groups. Asterisks indicate significance level. *$P < 0.05$; **$P < 0.01$; ***$P < 0.001$.

Kolyma (Fig. 5). In contrast, no signs of demographic expansion were detected by either test in the West Beringian phylogroup, which was instead characterized by high nucleotide diversity and relatively constant population effective size with some gradual increase over the last 60 kyr (Fig. 5 and Table 1). Compared with mitogenome diversity (Table 1), differences in nuclear genome diversity across the Eurasian phylogeographic groups are smaller (*SI Appendix*, Table S3). The highest RAD diversity estimates in the Taymyr group reflect ancient admixture as revealed by the coancestry matrix (Fig. 4). Consistent with differences in mitogenome nucleotide diversity, nuclear genome diversity in the West Beringian phylogroup tends to exceed estimates in the 2 Eurasian regions (Y, YK) without signs of population admixture.

In contrast to the high genetic diversity in the West Beringian phylogroup, mitogenome samples in the 4 regions (P, Y, T, YK) to the west of the Kolyma River demonstrated low nucleotide diversity, signs of demographic expansion, and recent time of common ancestry, with the earliest estimate around the Pleistocene-to-Holocene transition at 11.5 kyr. The lower mitogenome diversity suggests different demographic history, namely a smaller historical effective population size within the 4 regions across the Eurasian Arctic, compared with West Beringia. This difference in demographic history cannot be directly attributed to the impact of the last glaciation, as most of the Eurasian Arctic was not glaciated (34). It was suggested that the low mtDNA diversity resulted from regional bottleneck events due to the northward forest expansion contracting suitable tundra habitats to the west of the Kolyma River during Holocene warming (12, 13). Pollen and plant macrofossil records show that, over a large part of northern Eurasia, forest expanded to or near the Arctic coastline between 10 and 3 kyr during the Holocene thermal maximum (35–38). The significant impact of Holocene warming on the lemming's demographic history is supported by the present study. The species distribution models predict at least 25% habitat loss during the Middle Holocene compared with the present collared lemming distribution and, relative to the last glacial maximum, about 70% of habitat was lost across the Palearctic (*SI Appendix*, Fig. S2). Our analysis of demographic history based on mitogenome sequences (Fig. 5) detected a sudden increase in effective size at 4 to 2 kyr in the 3 regions (Y, T, YK) that were affected by forest advances, and timing of this population growth is consistent with tree line retreat to the current position and expansion of tundra biome at 3 kyr during the Late Holocene cooling (37). The significance of the Holocene environmental changes is further supported by the high mitogenome diversity indicating a constantly large population size in West Beringia where, in contrast to the rest of the Eurasian Arctic, little change in the position of the tree line was detected (36) and tundra landscape dominated throughout the Holocene (16, 35).

A recent paleogenetic study in a single population of the collared lemming from the Pechora region detected a drastic decrease in mtDNA diversity after the last glacial maximum (22 kyr) and over the Holocene that implies a pronounced demographic reduction (14). In this region, forest arrived at the coast (39) and fossils of the collared lemming were replaced by remains of taiga forest rodents between 8 and 4.5 kyr during the Holocene thermal optimum (40). These results support our inference that the low mitogenome diversity in the modern Pechora population reflects a decrease in effective size due to northward forest expansion contracting tundra habitats during the Holocene warming. Our study shows that the impact of the Holocene warming was not limited to a local scale but reduced the genetic diversity and population size of cold-adapted species in most geographic regions over the Eurasian Arctic, with the exception of West Beringia.

In conclusion, this study shows that environmental change during the Late Quaternary climate-warming events contracted distribution range, reduced effective population size, and decreased genetic diversity in an Arctic specialist, the collared lemming, across northern Eurasia. As supported by the ancestral phylogenetic position of the West Beringian group and the divergence time estimates of the other Eurasian clades, West Beringia was likely the single refugium during the continental range contraction caused by the high-magnitude climate warming of the last interglacial, followed by westward recolonization of northern Eurasia in the last glacial period. In line with these results, the highest mitogenome diversity was found in West Beringia and our demographic reconstruction indicates a constantly large effective population size thriving in this area over the last 60 kyr. It is likely that northward forest expansion over tundra during the Holocene thermal optimum did not affect the collared lemming in West Beringia while it reduced genomic diversity and effective population size in all other regions of the Eurasian Arctic. Under forecasted moderate climate warming, predicted habitat loss by 2080 for the collared lemming (41), a keystone species in the food web of Arctic communities, is comparable to range contraction during the last interglacial. Our study highlights the importance of West Beringia as a potential refugium for cold-adapted species

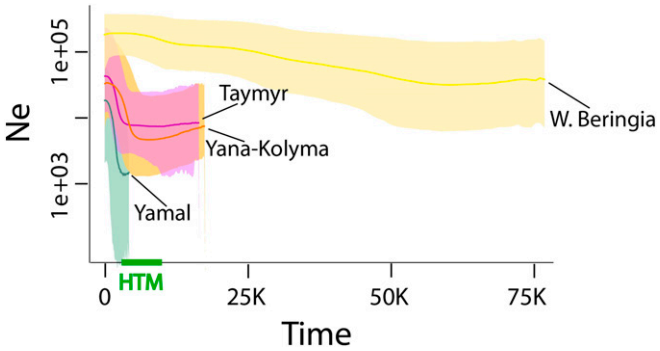

Fig. 5. Bayesian skyline plot based on mitogenome sequences showing effective size (N_e) changes through time in phylogeographic groups of collared lemmings. The green bar on the time scale indicates the warming period of the Holocene thermal maximum (HTM) (10 to 3 kyr).

under ongoing global warming. This conclusion is supported by recent paleoecological evidence suggesting a smaller temperature increase and moderate northward forest advances in the extreme northeast of Eurasia during the Late Pleistocene-to-Holocene warming events (16).

Materials and Methods

Sample Collection and DNA Extraction. We collected lemmings (*Dicrostonyx torquatus*, Pallas) across the Eurasian Arctic in the summers of 1994, 2002, and 2006 (Fig. 1). All tissue samples were deposited in the Mammal Collection, University of Alaska Museum of the North, from where additional tissue samples of North American lemmings (*D. groenlandicus*, Traill) were obtained to be included as an outgroup (*SI Appendix*, Table S1). Total genomic DNA was isolated from frozen or ethanol-preserved tissues by the use of the QIAGEN DNeasy Kit.

Mitochondrial Genomic Amplification and Sequencing. Complete mitochondrial genome (16,348 bp) sequences were obtained by amplification with PCR and capillary sequencing of amplified segments from both directions. A total of 16 pairs of primers (available on request) were designed for PCR amplification and sequencing. Annotated reference mitogenome assemblies were previously described (42, 43). We sequenced 54 mitogenomes of the Eurasian *D. torquatus* and genomes of 6 individuals of the North American *D. groenlandicus*.

RAD-Sequencing Data. Thirty-one individuals of *D. torquatus* from Eurasia (8 individuals each from West Beringia, Yana-Kolyma, and Yamal, and 7 from Taymyr) and 4 *D. groenlandicus* from Alaska were selected for reduced-representation genomic analysis due to higher DNA quality. Double-barcoded RAD-sequencing libraries were prepared following the protocol in Baird et al. (44) with modifications (45) and paired-end 125-bp sequenced (HiSeq 2500; V4 chemistry) at the Norwegian Sequencing Centre, University of Oslo.

After quality filtering, demultiplexing, and PCR-duplicate removal, sequenced reads were then de novo aligned into loci and single-nucleotide polymorphisms (SNPs) called across individuals using the script denovo_map.pl in the Stacks package version 1.48 (46). Settings for assembly parameters were tweaked to take into account the high genetic diversity of populations ranging across a broad geographical area and of different species (47, 48). Assembled loci were extracted from the catalog and quality-filtered (49). After excluding low-coverage samples with more than 25% missing loci, we generated a dataset including 15,619 loci genotyped in 26 *D. torquatus* samples, with a maximum 27% missing loci per individual and 24% missing genotypes per locus (Dataset Dtorquatus.txt). Genotype data for the low-coverage samples, where available, and for the 4 *D. groenlandicus* samples were then added to this dataset (Dataset Dicrostonyx.txt) to be used in the Neighbor-Net and TreeMix analyses (see *SI Appendix* for further details).

Analysis of Mitogenome Sequences. We conducted phylogenetic analysis of all mitochondrial genome sequences by using a coalescence-based approach as implemented in the software BEAST version 2.3 (50). The Yule tree prior was selected as suggested for interspecific phylogeny (50). After using ModelTest to find the simplest model of nucleotide substitution with good fit to the data on the basis of the Bayesian information criterion (51), we chose the HKY model with gamma-distributed rate variation. We assumed a strict molecular clock model, as preliminary analyses using a relaxed uncorrelated log-normal clock showed that the coefficient of log rate variation on branches (0.07) was smaller than 0.1 (52). To assess approximate timing of events in demographic history, we calibrated a molecular clock by placing a log-normal prior on the root of the tree, representing the divergence between the Eurasian *D. torquatus* and North American *D. groenlandicus* with the mean of 760 kyr as the first occurrence of the fossil record in North America (18, 19) and 95% CIs from 620 kyr to 1.1 My. We conducted 2 independent runs with 80 million iterations each, sampling from the posterior every 1,000 iterations and discarding the first 10% of sampled iterations as burn-in. Parameter mixing and convergence of the chains on a stationary distribution were assessed with Tracer version 1.6 (53). We obtained a maximum clade-credibility tree by use of TreeAnnotator and visualized the tree with FigTree version 1.3.1 (54). A Bayesian discrete phylogeography analysis was used to reconstruct the ancestral state and possible source of continental migration of the Eurasian lemmings as outlined in Faria et al. (55), coding the geographic location of all samples as a discrete trait and setting its substitution model as symmetric to allow reversible transition rates between locations. Three independent runs of 100 million iterations each were run in BEAST 1.10 (56). For each internal node, we obtained the posterior of each discrete state for the location trait and calculated the Bayes factor between the state with the highest posterior and all other states in pairwise comparisons. To analyze changes in relative population sizes over time, we reconstructed demographic histories independently in 4 phylogeographic groups (Y, T, YK, and WB) by using the Bayesian skyline plot (57) as implemented in Tracer version 1.6, with the substitution rate informed by phylogenetic analysis and the mean generation time of 1 y. Haplotype, nucleotide diversities, and demographic history statistics (33, 58) were calculated using DnaSP version 5 (59).

Analysis of RAD-Sequencing Data. To reveal the relationships among all individuals of the Eurasian *D. torquatus* relative to the North American outgroup *D. groenlandicus*, we built a Neighbor-Net (60) based on pairwise uncorrected *p* distances among samples. The generalization of a phylogenetic network, as compared with a tree, is an advantage when a set of multiple loci could have conflicting histories (e.g., due to recombination, admixture, etc.). Considering only the variable sites, we concatenated all loci for each individual in 2 sequences, randomly choosing the alternative alleles at heterozygous loci. Each individual is then represented by 2 tips in the resulting Neighbor-Net, where summed branch length separating them is proportional to individual heterozygosity. In the population under HW equilibrium, we expect the 2 tips representing an individual to be as far apart as any other tip from the same population. As this method is robust to missing data, we used the Dicro dataset, which includes also the genotypes of the low-coverage individuals as well as the 4 *D. groenlandicus* samples as an outgroup. The software SplitsTree4 (61) was used to build the Neighbor-Net. In addition, we used allele frequency data estimated on 1 randomly selected SNP per locus in the Dicro dataset to infer the pattern of splits and mixtures among the Eurasian phylogroups as identified in previous analyses. To account for secondary contacts and/or migrations among diverged populations while reconstructing the relationships among the sampled populations, we used the method implemented in TreeMix (62). The North American *D. groenlandicus* was set as an outgroup and the likelihood of models including from 0 to 5 migration events was estimated. The genetic structure across the Eurasian Arctic was also analyzed using the recently developed fineRADstructure (version 0.2) software package (63). Taking advantage of linked SNPs in each locus of the Dtorq dataset, we built a coancestry matrix of the 26 *D. torquatus* individuals. The nucleotide differences between the alleles of each individual and the alleles found in all of the other individuals at each locus were estimated and a coancestry matrix summarizing the nucleotide differences among individuals across all loci was constructed. We ran the scripts RADpainter and fineSTRUCTURE using default settings (http://cichlid.gurdon.cam.ac.uk/fineRADstructure.html).

The average number of polymorphic sites per locus, expected heterozygosity (H_e), Watterson's theta (θ_W), and nucleotide diversity (π) were estimated in each of the 4 Eurasian groups using the Dtorq dataset. Summary statistics were calculated for each locus and then averaged across all loci. In order to obtain estimates unbiased by sample size in each population, genetic diversity statistics were calculated by selecting at random 4 individuals per population at each locus. Loci with less than 4 individuals genotyped in a particular population were not included in the estimates concerning that population.

Species Distribution Modeling. Species distribution models (SDMs) were made via both current and past climate data at 2.5′ (4-km) spatial resolution, based on bioclimatic variables from the WorldClim dataset (64) (version 1.4). The last glacial maximum (LGM) climate data are derived from CMIP5 and utilize 3 general circulation model simulations: NCAR-CCSM, version 4.0; MIROC, version ESM 2010; and MPI, version ESM-LR. The last interglacial (LIG) climate data are derived from only the CCSM model (65). We compiled geospatial occurrences of *D. torquatus* collected by the authors. Because it has been shown that spatial sampling bias can result in overfit models (66–68), we removed redundant geolocations within 20 km, resulting in 21 occurrences used in modeling.

We used Maxent (version 3.3.3k) to first build SDMs of the present day and then project these models to past climates. The projection of species distributions to past or future climates has been criticized (69, 70), notably when models are overly fitted to present-day climates and then projected across timescales (71, 72). Thus, we utilized a number of measures to attempt to model the fundamental niche (70, 73). Besides pruning occurrences, we constructed present-day SDMs in a mask (40E–168W; 48N–85N) to avoid areas where congeners are absent, presumably for nonclimatic reasons (74, 75). We also removed correlated variables (Pearson's correlation coefficient $R^2 > 0.8$) among the 19 WorldClim variables to avoid overly complex models. Because parameter tuning can reduce overfitting and improve model performance (69), we optimized the regularization parameter (76), which penalizes the model proportional to the variance of features observed at presence localities and also inversely proportional to the square root of sample sizes (77). We

found the optimal regularization value (testing 1, 3, 5, 7, 9, 11, 13, and 15) using ENMTools version 1.3 (78), holding features constant.

With optimized model parameters, we first projected the present-day SDM, having a limited extent, onto the entire Palearctic region also for present-day climate. The SDM was next projected to past periods. All model outputs shown are averages of 5 replicates using the "cross-validate" option, with pixels receiving a continuous output score of between 0 and 1 indicating habitat suitability. For map calculations, we converted the outputs to binary predictions (suitable or unsuitable) but using 2 thresholds: minimum training presence or low, and equal training sensitivity and specificity or high (73). For the LGM and Middle Holocene timescales with multiple model simulations, we mapped habitat considered suitable by all 3 climate models used under both low and high thresholds. Arc Calculator in ArcGIS 10.0 was used for summing SDM outputs and calculating numbers of suitable pixels for each timescale. From these calculations, we estimated the percent of habitat loss in the LIG relative to both the present day and the LGM, as well as the percent of habitat loss in the Middle Holocene relative to both the present day and the LGM for the entire Eurasian Arctic.

Data Availability Statement. The DNA sequences were deposited in the NCBI GenBank database (*SI Appendix*, Table S1).

ACKNOWLEDGMENTS. Research reported in this publication was supported by grants (to V.B.F.) from the National Science Foundation (10.13039/100000001) (EPS-0346770), an Institutional Development Award from the National Institute of General Medical Sciences of the NIH (Grant 10.13039/100000057) (P20GM103395), Centre of Biomedical Research Excellence (Grant P20GM130443), and core funding of the Centre for Ecological and Evolutionary Synthesis, University of Oslo. The content is solely the responsibility of the authors and does not necessarily reflect the official views of the NIH. V.B.F. acknowledges logistical support for most of the field sampling from the Swedish Research Secretariat and J. A. Cook, Museum of Southwestern Biology, University of New Mexico, with the Beringian Coevolution Project. We thank G. H. Jarrell and L. E. Olson, Mammal Collection, University of Alaska Museum of the North, for providing tissue samples, R. Cristofari for help with RAD sequencing in the laboratory, and L. Dalen for discussing results.

1. T. V. Callaghan *et al*., Past changes in Arctic terrestrial ecosystems, climate and UV radiation. *Ambio* **33**, 398–403 (2004).
2. E. Post *et al*., Ecological dynamics across the Arctic associated with recent climate change. *Science* **325**, 1355–1358 (2009).
3. O. Gilg *et al*., Climate change and the ecology and evolution of Arctic vertebrates. *Ann. N. Y. Acad. Sci.* **1249**, 166–190 (2012).
4. R. Cristofari *et al*., Climate-driven range shifts of the king penguin in a fragmented ecosystem. *Nat. Clim. Chang.* **8**, 245–251 (2018).
5. CAPE-Last Interglacial Project Members, Last interglacial Arctic warmth confirms polar amplification of climate change. *Quat. Sci. Rev.* **25**, 1383–1400 (2006).
6. K. D. Bennett, *Evolution and Ecology: The Pace of Life* (Cambridge University Press, Cambridge, UK, 1997).
7. A. K. Agadjanian, "The history of collared lemmings in the Pleistocene" in *Beringia in the Cenozoic Era*, V. I. Kontrimavichus, Ed. (Academy of Science of USSR, Vladivostok, USSR, 1976), pp. 289–295.
8. V. S. Zazhigin, "Early evolutionary stages of collared lemmings (Dicrostonychini, Microtinae, Rodentia) as characteristic representatives of Beringian subarctic fauna" in *Beringia in the Cenozoic Era*, V. I. Kontrimavichus, Ed. (Academy of Science of USSR, Vladivostok, USSR, 1976), pp. 280–288.
9. K. Kowalski, Lemmings (Mammalia, Rodentia) as indicators of temperature and humidity in the European Quaternary. *Acta Zoolika Cracovenzis* **38**, 85–94 (1995).
10. F. A. Pitelka, G. O. Batzli, "Distribution, abundance and habitat use by lemmings on the north slope of Alaska" in *The Biology of Lemmings*, N. C. Stenseth, R. A. Ims, Eds. (Academic Press, London, UK, 1993), pp. 214–234.
11. A. K. Markova *et al*., Late Pleistocene distribution and diversity of mammals in northern Eurasia. *Paleontologia i Evolucia* **28–29**, 5–143 (1995).
12. V. B. Fedorov, Contrasting mitochondrial DNA diversity estimates in two sympatric genera of Arctic lemmings (*Dicrostonyx, Lemmus*) indicate different responses to Quaternary environmental fluctuations. *Proc. Biol. Sci.* **266**, 621–626 (1999).
13. V. B. Fedorov, K. Fredga, G. Jarrell, Mitochondrial DNA variation and the evolutionary history of chromosome races of collared lemmings (*Dicrostonyx*) in the Eurasian Arctic. *J. Evol. Biol.* **12**, 134–145 (1999).
14. S. Prost *et al*., Influence of climate warming on Arctic mammals? New insights from ancient DNA studies of the collared lemming *Dicrostonyx torquatus*. *PLoS One* **5**, e10447 (2010).
15. E. Palkopoulou *et al*., Synchronous genetic turnovers across western Eurasia in Late Pleistocene collared lemmings. *Glob. Change Biol.* **22**, 1710–1721 (2016).
16. P. E. Tarasov *et al*., A pollen based biome reconstruction over the last 3.562 million years in the Far East Russian Arctic—New insights into climate-vegetation relationships at the regional scale. *Clim. Past* **9**, 2759–2775 (2013).
17. V. B. Fedorov, A. V. Goropashnaya, The importance of ice ages in diversification of Arctic collared lemmings (*Dicrostonyx*): Evidence from the mitochondrial cytochrome *b* region. *Hereditas* **130**, 301–307 (1999).
18. C. R. Harington, "Ice age vertebrates in the Canadian Arctic islands" in *Canada's Missing Dimension: Science and History in the Canadian Arctic Islands*, C. R. Harington, Ed. (Canadian Museum of Nature, Ottawa, Canada, 1990), pp. 140–160.
19. C. R. Harington, Pleistocene vertebrates of the Yukon Territory. *Quat. Sci. Rev.* **30**, 2341–2354 (2011).
20. R. D. Guthrie, J. V. Matthews, Jr, The Cape Deceit fauna Early Pleistocene mammalian assemblage from the Alaskan Arctic. *Quat. Res.* **1**, 474–510 (1971).
21. J. E. Storer, The eastern Beringian vole *Microtus deceitensis* (Rodentia, Muridae, Arvicolinae) in Late Pliocene and Early Pleistocene faunas of Alaska and Yukon. *Quat. Res.* **60**, 84–93 (2003).
22. S. Y. W. Ho, M. J. Phillips, A. Cooper, A. J. Drummond, Time dependency of molecular rate estimates and systematic overestimation of recent divergence times. *Mol. Biol. Evol.* **22**, 1561–1568 (2005).
23. J. S. Herman, J. B. Searle, Post-glacial partitioning of mitochondrial genetic variation in the field vole. *Proc. Biol. Sci.* **278**, 3601–3607 (2011).
24. N. Martínková *et al*., Divergent evolutionary processes associated with colonization of offshore islands. *Mol. Ecol.* **22**, 5205–5220 (2013).
25. A. Dutton *et al*., SEA-LEVEL RISE. Sea-level rise due to polar ice-sheet mass loss during past warm periods. *Science* **349**, aaa4019 (2015).
26. V. P. Grichuk, "Late Pleistocene vegetation history" in *Late Quaternary Environments of the Soviet Union*, A. A. Velichko, Ed. (University of Minnesota Press, Minneapolis, MN, 1984), pp. 155–178.
27. T. D. Morozova, A. A. Velichko, K. G. Dlussky, Organic carbon content in the Late Pleistocene and Holocene fossil soils (reconstruction for eastern Europe). *Global Planet. Change* **16–17**, 131–151 (1998).
28. A. V. Lozhkin, P. M. Anderson, The last interglaciation of northeast Siberia. *Quat. Res.* **43**, 147–158 (1995).
29. F. Kienast *et al*., Paleontological records indicate the occurrence of open woodlands in a dry inland climate at the present-day Arctic coast in western Beringia during the last interglacial. *Quat. Sci. Rev.* **30**, 2134–2159 (2011).
30. A. V. Sher, Problems of the interglacial in Arctic Siberia. *Quat. Int.* **10–12**, 215–222 (1991).
31. M. Melles *et al*., 2.8 million years of Arctic climate change from Lake El'gygytgyn, NE Russia. *Science* **337**, 315–320 (2012).
32. A. V. Lozhkin, P. M. Anderson, T. Matrosova, P. Minyuk, The pollen record from El'gygytgyn Lake: Implications for vegetation and climate histories of northern Chukotka since the Late Middle Pleistocene. *J. Paleolimnol.* **37**, 135–153 (2007).
33. S. E. Ramos-Onsins, J. Rozas, Statistical properties of new neutrality tests against population growth. *Mol. Biol. Evol.* **19**, 2092–2100 (2002).
34. J. I. Svendsen *et al*., Late Quaternary ice sheet history of northern Eurasia. *Quat. Sci. Rev.* **23**, 1229–1271 (2004).
35. N. H. Bigelow *et al*., Climate change and Arctic ecosystems: 1. Vegetation changes north of 55 N between the last glacial maximum, Mid-Holocene, and present. *J. Geophys. Res.* **108**, 8170 (2003).
36. H. A. Binney *et al*., The distribution of Late-Quaternary woody taxa in northern Eurasia: Evidence from a new macrofossil database. *Quat. Sci. Rev.* **28**, 2445–2464 (2009).
37. G. M. MacDonald *et al*., Holocene treeline history and climate change across northern Eurasia. *Quat. Res.* **53**, 302–311 (2000).
38. S. Payette, M. Eronen, J. J. P. Jasinski, The circumboreal tundra-taiga interface: Late Pleistocene and Holocene changes. *Ambio* **12**, 15–22 (2002).
39. J. S. Salonen *et al*., The Holocene thermal maximum and Late-Holocene cooling in the tundra of NE European Russia. *Quat. Res.* **75**, 501–511 (2011).
40. I. B. Golovachov, N. G. Smirnov, The Late Pleistocene and Holocene rodents of the pre-Urals subarctic. *Quat. Int.* **201**, 37–42 (2009).
41. S. Prost *et al*., Losing ground: Past history and future fate of Arctic small mammals in a changing climate. *Glob. Change Biol.* **16**, 1854–1864 (2013).
42. V. B. Fedorov, A. V. Goropashnaya, Complete mitochondrial genomes of the North American collared lemmings *Dicrostonyx groenlandicus* Traill, 1823 and *Dicrostonyx hudsonius* Pallas, 1778 (Rodentia: Arvicolinae). *Mitochondrial DNA B Resour.* **1**, 878–879 (2016).
43. V. B. Fedorov, A. V. Goropashnaya, Complete mitochondrial genome of the Eurasian collared lemming *Dicrostonyx torquatus* Pallas, 1779 (Rodentia: Arvicolinae). *Mitochondrial DNA B Resour.* **1**, 824–825 (2016).
44. N. A. Baird *et al*., Rapid SNP discovery and genetic mapping using sequenced RAD markers. *PLoS One* **3**, e3376 (2008).
45. R. Cristofari *et al*., Full circumpolar migration ensures evolutionary unity in the emperor penguin. *Nat. Commun.* **7**, 11842 (2016).
46. J. Catchen, P. A. Hohenlohe, S. Bassham, A. Amores, W. A. Cresko, Stacks: An analysis tool set for population genomics. *Mol. Ecol.* **22**, 3124–3140 (2013).
47. P. Gratton *et al*., Testing classical species properties with contemporary data: How "bad species" in the brassy ringlets (*Erebia tyndarus* complex, Lepidoptera) turned good. *Syst. Biol.* **65**, 292–303 (2016).
48. J. R. Paris, J. R. Stevens, J. M. Catchen, Lost in parameter space: A road map for Stacks. *Methods Ecol. Evol.* **8**, 1360–1373 (2017).
49. E. Trucchi, B. Frajman, T. H. A. Haverkamp, P. Schönswetter, O. Paun, Genomic analyses suggest parallel ecological divergence in *Heliosperma pusillum* (Caryophyllaceae). *New Phytol.* **216**, 267–278 (2017).
50. A. J. Drummond, R. R. Bouckaert, *Bayesian Evolutionary Analysis with BEAST* (Cambridge University Press, Cambridge, UK, 2015).
51. D. Posada, jModelTest: Phylogenetic model averaging. *Mol. Biol. Evol.* **25**, 1253–1256 (2008).

52. R. P. Brown, Z. Yang, Rate variation and estimation of divergence times using strict and relaxed clocks. *BMC Evol. Biol.* **11**, 271 (2011).
53. A. Rambaut, A. J. Drummond, Tracer, Version 1.6. http://beast.bio.ed.ac.uk. Accessed 7 January 2020.
54. A. Rambaut, FigTree, Version 1.3.1. http://tree.bio.ed.ac.uk/software/figtree. Accessed 7 January 2020.
55. N. R. Faria, M. A. Suchard, A. Rambaut, P. Lemey, Toward a quantitative understanding of viral phylogeography. *Curr. Opin. Virol.* **1**, 423–429 (2011).
56. M. A. Suchard *et al*., Bayesian phylogenetic and phylodynamic data integration using BEAST 1.10. *Virus Evol.* **4**, vey016 (2018).
57. J. Heled, A. J. Drummond, Bayesian inference of population size history from multiple loci. *BMC Evol. Biol.* **8**, 289 (2008).
58. Y. X. Fu, Statistical tests of neutrality of mutations against population growth, hitchhiking and background selection. *Genetics* **147**, 915–925 (1997).
59. P. Librado, J. Rozas, DnaSP v5: A software for comprehensive analysis of DNA polymorphism data. *Bioinformatics* **25**, 1451–1452 (2009).
60. D. Bryant, V. Moulton, Neighbor-Net: An agglomerative method for the construction of phylogenetic networks. *Mol. Biol. Evol.* **21**, 255–265 (2004).
61. D. H. Huson, D. Bryant, Application of phylogenetic networks in evolutionary studies. *Mol. Biol. Evol.* **23**, 254–267 (2006).
62. J. K. Pickrell, J. K. Pritchard, Inference of population splits and mixtures from genome-wide allele frequency data. *PLoS Genet.* **8**, e1002967 (2012).
63. M. Malinsky, E. Trucchi, D. J. Lawson, D. Falush, RADpainter and fineRADstructure: Population inference from RADseq data. *Mol. Biol. Evol.* **35**, 1284–1290 (2018).
64. R. J. Hijmans, S. E. Cameron, J. L. Parra, P. G. Jones, A. Jarvis, Very high resolution interpolated climate surfaces for global land areas. *Int. J. Climatol.* **25**, 1965–1978 (2005).
65. B. L. Otto-Bliesner *et al*., Last glacial maximum and Holocene climate in CCSM3. *J. Clim.* **19**, 2526–2544 (2006).
66. S. Reddy, L. M. Dávalos, Geographical sampling bias and its implications for conservation priorities in Africa. *J. Biogeogr.* **30**, 1719–1727 (2003).
67. S. D. Veloz, Spatially autocorrelated sampling falsely inflates measures of accuracy for presence-only niche models. *J. Biogeogr.* **36**, 2290–2299 (2009).
68. S. Kramer-Schadt *et al*., The importance of correcting for sampling bias in MaxEnt species distribution models. *Divers. Distrib.* **19**, 1366–1379 (2013).
69. R. P. Anderson, I. Gonzalez, Jr, Species-specific tuning increases robustness to sampling bias in models of species distributions: An implementation with Maxent. *Ecol. Modell.* **222**, 2796–2811 (2011).
70. A. T. Peterson *et al*., *Ecological Niches and Geographic Distributions (MPB-49)* (Princeton University Press, Princeton, NJ, 2011).
71. E. B. Davis, J. L. McGuire, J. D. Orcutt, Ecological niche models of mammalian glacial refugia show consistent bias. *Ecography* **37**, 1133–1138 (2014).
72. J. R. P. Worth, G. J. Williamson, S. Sakaguchi, P. G. Nevill, G. J. Jordan, Environmental niche modelling fails to predict last glacial maximum refugia: Niche shifts, micro-refugia or incorrect palaeoclimate estimates? *Glob. Ecol. Biogeogr.* **23**, 1186–1197 (2014).
73. A. G. Hope *et al*., Arctic biodiversity: Increasing richness accompanies shrinking refugia for a cold-associated tundra fauna. *Ecosphere* **6**, 159 (2015).
74. R. P. Anderson, A. Raza, The effect of the extent of the study region on GIS models of species geographic distributions and estimates of niche evolution: Preliminary tests with montane rodents (genus Nephelomys) in Venezuela. *J. Biogeogr.* **37**, 1378–1393 (2010).
75. N. Barve *et al*., The crucial role of the accessible area in ecological niche modeling and species distribution modeling. *Ecol. Modell.* **222**, 1810–1819 (2011).
76. D. L. Warren, S. N. Seifert, Ecological niche modeling in Maxent: The importance of model complexity and the performance of model selection criteria. *Ecol. Appl.* **21**, 335–342 (2011).
77. C. Merow, M. J. Smith, J. A. Silander, A practical guide to MaxEnt for modeling species' distributions: What it does, and why inputs and settings matter. *Ecography* **36**, 1058–1069 (2013).
78. D. L. Warren, R. E. Glor, M. Turelli, ENMTools: A toolbox for comparative studies of environmental niche models. *Ecography* **33**, 607–611 (2010).